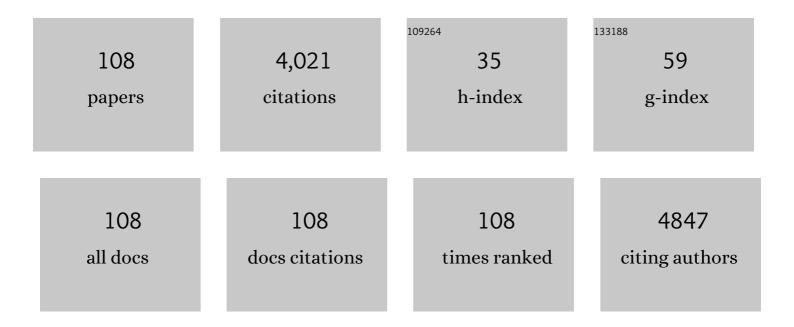
Svemir Rudic

List of Publications by Year in descending order

Source: https://exaly.com/author-pdf/8628542/publications.pdf Version: 2024-02-01



#	Article	IF	CITATIONS
1	Selective Adsorption of Sulfur Dioxide in a Robust Metal–Organic Framework Material. Advanced Materials, 2016, 28, 8705-8711.	11.1	214
2	Identifying the Role of Terahertz Vibrations in Metal-Organic Frameworks: From Gate-Opening Phenomenon to Shear-Driven Structural Destabilization. Physical Review Letters, 2014, 113, 215502.	2.9	202
3	Confinement of Iodine Molecules into Triple-Helical Chains within Robust Metal–Organic Frameworks. Journal of the American Chemical Society, 2017, 139, 16289-16296.	6.6	199
4	Reversible coordinative binding and separation of sulfur dioxide in a robust metal–organic framework with open copper sites. Nature Materials, 2019, 18, 1358-1365.	13.3	171
5	Breaking the Limit of Lignin Monomer Production via Cleavage of Interunit Carbon–Carbon Linkages. CheM, 2019, 5, 1521-1536.	5.8	167
6	Inelastic neutron scattering study of reline: shedding light on the hydrogen bonding network of deep eutectic solvents. Physical Chemistry Chemical Physics, 2017, 19, 17998-18009.	1.3	132
7	Recent and future developments on TOSCA at ISIS. Journal of Physics: Conference Series, 2014, 554, 012003.	0.3	126
8	Inside PEF: Chain Conformation and Dynamics in Crystalline and Amorphous Domains. Macromolecules, 2018, 51, 3515-3526.	2.2	110
9	Paving the way for methane hydrate formation on metal–organic frameworks (MOFs). Chemical Science, 2016, 7, 3658-3666.	3.7	103
10	A comprehensive approach to investigate the structural and surface properties of activated carbons and related Pd-based catalysts. Catalysis Science and Technology, 2016, 6, 4910-4922.	2.1	96
11	Integration of mesopores and crystal defects in metal-organic frameworks via templated electrosynthesis. Nature Communications, 2019, 10, 4466.	5.8	90
12	The neutron guide upgrade of the TOSCA spectrometer. Nuclear Instruments and Methods in Physics Research, Section A: Accelerators, Spectrometers, Detectors and Associated Equipment, 2018, 896, 68-74.	0.7	84
13	Modulating supramolecular binding of carbon dioxide in a redox-active porous metal-organic framework. Nature Communications, 2017, 8, 14212.	5.8	75
14	Quantitative production of butenes from biomass-derived γ-valerolactone catalysed by hetero-atomic MFI zeolite. Nature Materials, 2020, 19, 86-93.	13.3	74
15	Pore Distortion in a Metal–Organic Framework for Regulated Separation of Propane and Propylene. Journal of the American Chemical Society, 2021, 143, 19300-19305.	6.6	72
16	The dynamics of formation of HCl products from the reaction of Cl atoms with methanol, ethanol, and dimethyl ether. Journal of Chemical Physics, 2002, 117, 5692-5706.	1.2	69
17	On-the-flyab initiotrajectory calculations of the dynamics of Cl atom reactions with methane, ethane and methanol. Journal of Chemical Physics, 2004, 120, 186-198.	1.2	69
18	Graphitization of Activated Carbons: A Molecular-level Investigation by INS, DRIFT, XRD and Raman Techniques. Physics Procedia, 2016, 85, 20-26.	1.2	68

#	Article	IF	CITATIONS
19	High Ammonia Adsorption in MFM-300 Materials: Dynamics and Charge Transfer in Host–Guest Binding. Journal of the American Chemical Society, 2021, 143, 3153-3161.	6.6	67
20	Atomically Dispersed Copper Sites in a Metal–Organic Framework for Reduction of Nitrogen Dioxide. Journal of the American Chemical Society, 2021, 143, 10977-10985.	6.6	66
21	Detecting Molecular Rotational Dynamics Complementing the Low-Frequency Terahertz Vibrations in a Zirconium-Based Metal-Organic Framework. Physical Review Letters, 2017, 118, 255502.	2.9	60
22	Direct Evidence for Solid-like Hydrogen in a Nanoporous Carbon Hydrogen Storage Material at Supercritical Temperatures. ACS Nano, 2015, 9, 8249-8254.	7.3	57
23	Observation of Binding and Rotation of Methane and Hydrogen within a Functional Metal–Organic Framework. Journal of the American Chemical Society, 2016, 138, 9119-9127.	6.6	54
24	Structural dynamics of a metal–organic framework induced by CO2 migration in its non-uniform porous structure. Nature Communications, 2019, 10, 999.	5.8	54
25	Unexpected Cation Dynamics in the Low-Temperature Phase of Methylammonium Lead Iodide: The Need for Improved Models. Journal of Physical Chemistry Letters, 2016, 7, 4701-4709.	2.1	53
26	Predicting the reactivity of energetic materials: an <i>ab initio</i> multi-phonon approach. Journal of Materials Chemistry A, 2019, 7, 19539-19553.	5.2	52
27	Purification of Propylene and Ethylene by a Robust Metal–Organic Framework Mediated by Host–Guest Interactions. Angewandte Chemie - International Edition, 2021, 60, 15541-15547.	7.2	51
28	Host–guest selectivity in a series of isoreticular metal–organic frameworks: observation of acetylene-to-alkyne and carbon dioxide-to-amide interactions. Chemical Science, 2019, 10, 1098-1106.	3.7	47
29	Understanding the ZIF-L to ZIF-8 transformation from fundamentals to fully costed kilogram-scale production. Communications Chemistry, 2022, 5, .	2.0	45
30	Infrared laser spectroscopy of CH3â< HF in helium nanodroplets: The exit-channel complex of the F+CH4 reaction. Journal of Chemical Physics, 2006, 124, 084301.	1.2	44
31	Rotational distribution of the HCl products from the reaction of Cl(2P) atoms with methanol. Chemical Physics Letters, 2000, 332, 487-495.	1.2	43
32	Sources of Error and Uncertainty in the Use of Cavity Ring Down Spectroscopy to Measure Aerosol Optical Properties. Aerosol Science and Technology, 2011, 45, 1360-1375.	1.5	43
33	The product branching and dynamics of the reaction of chlorine atoms with methylamine. Physical Chemistry Chemical Physics, 2003, 5, 1205-1212.	1.3	41
34	Influence of Uncertainties in the Diameter and Refractive Index of Calibration Polystyrene Beads on the Retrieval of Aerosol Optical Properties Using Cavity Ring Down Spectroscopy. Journal of Physical Chemistry A, 2010, 114, 7077-7084.	1.1	41
35	Stereodynamics of Chlorine Atom Reactions with Organic Molecules. Journal of Physical Chemistry A, 2005, 109, 11093-11102.	1.1	39
36	Measurements of the wavelength dependent extinction of aerosols by cavity ring down spectroscopy. Physical Chemistry Chemical Physics, 2010, 12, 3914.	1.3	39

#	Article	IF	CITATIONS
37	Nuclear dynamics and phase polymorphism in solid formic acid. Physical Chemistry Chemical Physics, 2017, 19, 9064-9074.	1.3	33
38	Unusual flexibility of mesophase pitch-derived carbon materials: An approach to the synthesis of graphene. Carbon, 2017, 115, 539-545.	5.4	31
39	Carbohydrate hydration: heavy water complexes of α and β anomers of glucose, galactose, fucose and xylose. Physical Chemistry Chemical Physics, 2011, 13, 18671.	1.3	29
40	Emergence of glassy features in halomethane crystals. Physical Review B, 2019, 99, .	1.1	29
41	Nonlinear effects in pulsed cavity ringdown spectroscopy of lithium vapour. Chemical Physics Letters, 2000, 320, 613-622.	1.2	28
42	Hydrogen Bond Dynamics of Cellulose through Inelastic Neutron Scattering Spectroscopy. Biomacromolecules, 2018, 19, 1305-1313.	2.6	28
43	Guest–host interactions of nanoconfined anti-cancer drug in metal–organic framework exposed by terahertz dynamics. Chemical Communications, 2019, 55, 3868-3871.	2.2	27
44	Effect of pore geometry on ultra-densified hydrogen in microporous carbons. Carbon, 2021, 173, 968-979.	5.4	25
45	Guest-Controlled Incommensurate Modulation in a Meta-Rigid Metal–Organic Framework Material. Journal of the American Chemical Society, 2020, 142, 19189-19197.	6.6	24
46	Asymmetric Monomer, Amorphous Polymer? Structure–Property Relationships in 2,4-FDCA and 2,4-PEF. Macromolecules, 2020, 53, 1380-1387.	2.2	24
47	Direct Observation of Ammonia Storage in UiO-66 Incorporating Cu(II) Binding Sites. Journal of the American Chemical Society, 2022, 144, 8624-8632.	6.6	24
48	Heavy water hydration of mannose: the anomeric effect in solvation, laid bare. Chemical Science, 2011, 2, 1128.	3.7	23
49	Water dynamics in MCF-7 breast cancer cells: a neutron scattering descriptive study. Scientific Reports, 2019, 9, 8704.	1.6	23
50	Control of zeolite microenvironment for propene synthesis from methanol. Nature Communications, 2021, 12, 822.	5.8	23
51	Progress in the Characterization of the Surface Species in Activated Carbons by means of INS Spectroscopy Coupled with Detailed DFT Calculations. Advances in Condensed Matter Physics, 2015, 2015, 1-8.	0.4	22
52	Direct observation of supramolecular binding of light hydrocarbons in vanadium(<scp>iii</scp>) and (<scp>iv</scp>) metal–organic framework materials. Chemical Science, 2018, 9, 3401-3408.	3.7	22
53	Detailed characterisation of the incident neutron beam on the TOSCA spectrometer. Nuclear Instruments and Methods in Physics Research, Section A: Accelerators, Spectrometers, Detectors and Associated Equipment, 2017, 870, 79-83.	0.7	22
54	The effect of surface chemistry on the performances of Pd-based catalysts supported on activated carbons. Catalysis Science and Technology, 2017, 7, 4162-4172.	2.1	21

#	Article	IF	CITATIONS
55	Vibrationally induced metallisation of the energetic azide α-NaN ₃ . Physical Chemistry Chemical Physics, 2018, 20, 29061-29069.	1.3	21
56	Infrared laser spectroscopy of the CH3–HCN radical complex stabilized in helium nanodroplets. Journal of Chemical Physics, 2006, 124, 104305.	1.2	20
57	Poly(4-styrene sulfonic acid)/bacterial cellulose membranes: Electrochemical performance in a single-chamber microbial fuel cell. Bioresource Technology Reports, 2020, 9, 100376.	1.5	20
58	Green Reconstruction of MIL-100 (Fe) in Water for High Crystallinity and Enhanced Guest Encapsulation. ACS Sustainable Chemistry and Engineering, 2020, 8, 8247-8255.	3.2	20
59	Conformational effects in sugar ions: spectroscopic investigations in the gas phase and in solution. Chemical Science, 2012, 3, 2307.	3.7	19
60	Monte carlo simulations of the TOSCA spectrometer: Assessment of current performance and future upgrades. EPJ Web of Conferences, 2015, 83, 03013.	0.1	19
61	Study of the CH3â< H2O radical complex stabilized in helium nanodroplets. Physical Chemistry Chemical Physics, 2009, 11, 5345.	1.3	17
62	Protonated sugars: vibrational spectroscopy and conformational structure of protonatedO-methyl α-D-galactopyranoside. Molecular Physics, 2012, 110, 1609-1615.	0.8	17
63	A New Look into the Mode of Action of Metal-Based Anticancer Drugs. Molecules, 2020, 25, 246.	1.7	17
64	Water in Deep Eutectic Solvents: New Insights From Inelastic Neutron Scattering Spectroscopy. Frontiers in Physics, 2022, 10, .	1.0	17
65	Optical properties of micrometer size water droplets studied by cavity ringdown spectroscopy. Applied Optics, 2007, 46, 6142.	2.1	16
66	Influence of Solvent on Poly(2-(Dimethylamino)Ethyl Methacrylate) Dynamics in Polymer-Concentrated Mixtures: A Combined Neutron Scattering, Dielectric Spectroscopy, and Calorimetric Study. Macromolecules, 2015, 48, 6724-6735.	2.2	16
67	Neutronic developments on TOSCA and VESPA: Progress to date. Physica B: Condensed Matter, 2019, 562, 107-111.	1.3	16
68	OX-1 Metal–Organic Framework Nanosheets as Robust Hosts for Highly Active Catalytic Palladium Species. ACS Sustainable Chemistry and Engineering, 2019, 7, 5875-5885.	3.2	15
69	Measurement of the para-hydrogen concentration in the ISIS moderators using neutron transmission and thermal conductivity. Nuclear Instruments and Methods in Physics Research, Section A: Accelerators, Spectrometers, Detectors and Associated Equipment, 2018, 888, 88-95.	0.7	14
70	The TOSCA Spectrometer at ISIS: the Guide Upgrade and Beyond. Journal of Physics: Conference Series, 2018, 1021, 012029.	0.3	14
71	Predicting the impact sensitivity of a polymorphic high explosive: the curious case of FOX-7. Chemical Communications, 2021, 57, 11213-11216.	2.2	14
72	Origin of natural and magnetic field induced polar order in orthorhombic PrFe1/2Cr1/2O3. Physical Review B, 2021, 104, .	1.1	14

#	Article	IF	CITATIONS
73	Confinement of poly(ethylene oxide) in the nanometer-scale pores of resins and carbon nanoparticles. Soft Matter, 2013, 9, 10960.	1.2	13
74	Intracellular water as a mediator of anticancer drug action. International Reviews in Physical Chemistry, 2020, 39, 67-81.	0.9	13
75	Intercalation and Confinement of Poly(ethylene oxide) in Porous Carbon Nanoparticles with Controlled Morphologies. Macromolecules, 2014, 47, 8729-8737.	2.2	12
76	Looking inside the pores of a MCM-41 based Mo heterogeneous styrene oxidation catalyst: an inelastic neutron scattering study. Physical Chemistry Chemical Physics, 2016, 18, 17272-17280.	1.3	12
77	CO ₂ Capture by Nickel Hydroxide Interstratified in the Nanolayered Space of a Synthetic Clay Mineral. Journal of Physical Chemistry C, 2020, 124, 26222-26231.	1.5	12
78	Understanding the Structure and Dynamics of Nanocellulose-Based Composites with Neutral and Ionic Poly(methacrylate) Derivatives Using Inelastic Neutron Scattering and DFT Calculations. Molecules, 2020, 25, 1689.	1.7	12
79	Direct Visualization of Supramolecular Binding and Separation of Light Hydrocarbons in MFM-300(In). Chemistry of Materials, 2022, 34, 5698-5705.	3.2	11
80	Determination of the scattering cross section of calcium using the VESUVIO spectrometer. Nuclear Instruments and Methods in Physics Research, Section A: Accelerators, Spectrometers, Detectors and Associated Equipment, 2019, 927, 443-450.	0.7	10
81	A HF Loaded Lewisâ€Acidic Aluminium Chlorofluoride for Hydrofluorination Reactions. Chemistry - A European Journal, 2020, 26, 7314-7322.	1.7	10
82	Ammonia Storage in Hydrogen Bond-Rich Microporous Polymers. ACS Applied Materials & Interfaces, 2020, 12, 58161-58169.	4.0	9
83	Volatile Hydrogen Intermediates of CO2 Methanation by Inelastic Neutron Scattering. Catalysts, 2020, 10, 433.	1.6	9
84	Dynamics of hydrogen guests in ice XVII nanopores. Physical Review Materials, 2017, 1, .	0.9	9
85	Dynamics and Structure of Poly(ethylene oxide) Intercalated in the Nanopores of Resorcinol–Formaldehyde Resin Nanoparticles. Macromolecules, 2016, 49, 5704-5713.	2.2	8
86	Molecular Insights into Bulk and Porous κ ² <i>P,N</i> â€PTA Metalâ€Organic Polymers by Simultaneous Raman Spectroscopy and Inelastic Neutron Scattering. European Journal of Inorganic Chemistry, 2019, 2019, 1155-1161.	1.0	7
87	Spontaneous formation of an ordered interstratification upon Ni-exchange of Na-fluorohectorite. Applied Clay Science, 2020, 198, 105831.	2.6	7
88	Metallodrug-protein interaction probed by synchrotron terahertz and neutron scattering spectroscopy. Biophysical Journal, 2021, 120, 3070-3078.	0.2	7
89	Positional, isotopic mass and force constant disorder in molybdate glasses and their parent metal oxides as observed by neutron diffraction and Compton scattering. Journal of Physics Communications, 2020, 4, 095027.	0.5	7
90	A tale of two foils: ISIS TS-1 water moderators. Journal of Physics: Conference Series, 2018, 1021, 012039.	0.3	6

#	Article	IF	CITATIONS
91	Discovery of new neutron-moderating materials at ISIS Neutron and Muon Source. EPJ Web of Conferences, 2020, 239, 17008.	0.1	6
92	High capacity ammonia adsorption in a robust metal–organic framework mediated by reversible host–guest interactions. Chemical Communications, 2022, 58, 5753-5756.	2.2	6
93	A Python Algorithm to Analyze Inelastic Neutron Scattering Spectra Based on the y-Scale Formalism. Journal of Chemical Theory and Computation, 2020, 16, 7671-7680.	2.3	5
94	Inelastic Neutron Scattering Investigation of MgCl ₂ Nanoparticle-Based Ziegler–Natta Catalysts for Olefin Polymerization. ACS Applied Nano Materials, 2020, 3, 11118-11128.	2.4	5
95	Secondary relaxation in the terahertz range in 2-adamantanone from theory and experiments. Physical Review B, 2020, 101, .	1.1	5
96	Human hair: subtle change in the thioester groups dynamics observed by combining neutron scattering, X-ray diffraction and thermal analysis. European Physical Journal: Special Topics, 2020, 229, 2825-2832.	1.2	5
97	Hydrogen bond dynamics and conformational flexibility in antipsychotics. Physical Chemistry Chemical Physics, 2019, 21, 15463-15470.	1.3	4
98	Probing the relevance of MoO ₂ nanoparticles' synthesis on their catalytic activity by inelastic neutron scattering. Physical Chemistry Chemical Physics, 2020, 22, 896-904.	1.3	4
99	Density of Phonon States in Cubic Ice Ic. Journal of Physical Chemistry C, 2021, 125, 23533-23538.	1.5	4
100	Interplay between Local Structure and Nuclear Dynamics in Tungstic Acid: A Neutron Scattering Study. Journal of Physical Chemistry C, 2021, 125, 23864-23879.	1.5	4
101	Spectroscopic Signatures of Hydrogen-Bonding Motifs in Protonic Ionic Liquid Systems: Insights from Diethylammonium Nitrate in the Solid State. Journal of Physical Chemistry C, 2021, 125, 24463-24476.	1.5	4
102	Crystal Analyzers for Indirect-Geometry Broadband Neutron Spectrometers: Adding Reality to Idealized Design. Journal of Surface Investigation, 2020, 14, S242-S250.	0.1	3
103	Understanding the effect of lattice polarisability on the electrochemical properties of lithium tetrahaloaluminates, LiAl <i>X</i> ₄ (<i>X</i> = Cl, Br, I). Journal of Materials Chemistry A, 0, .	5.2	3
104	Spin isomers in the ISIS TS1 cryogenic hydrogen moderator. Journal of Physics: Conference Series, 2018, 1021, 012057.	0.3	2
105	Robust measurement of para-ortho H ₂ ratios to characterise the ISIS hydrogen moderators. Journal of Physics: Conference Series, 2018, 1021, 012055.	0.3	2
106	Hydrogen Detection Limits and Instrument Sensitivity of High-Resolution Broadband Neutron Spectrometers. Analytical Chemistry, 2022, 94, 5023-5028.	3.2	2
107	Cryogenic sample environment on TOSCA. Journal of Physics: Conference Series, 2014, 554, 012007.	0.3	1
108	Spectroscopic Identification of Disordered Molecular Cations in Defect Perovskiteâ€like ALn(HCO2)(C2O4)1.5 (Ln = Tbâ€Er) Phases. European Journal of Inorganic Chemistry, 2021, 2021, 3806.	1.0	1